Archives of Environmental Protection
Vol. 45 no. 4 pp. 30–39

PL ISSN 2083-4772
DOI 10.24425/aep.2019.130239

Dye removal using keggin polyoxometalates assisted ultrafiltration: characterization and UV visible study

Malak Kahloul[1,2]*, Jalila Chekir[1], Amor Hafiane[1]

[1]Laboratory of Water, Membrane and Environmental Biotechnology
(LEMBE), CERTE BP 273, 8020 Soliman, Tunisia
[2]Faculty of Sciences of Tunis, University Tunis – El Manar
20 Tolede Street, Tunis 2092, Tunisia

*Corresponding author's e-mail: kahloul2.malak@gmail.com

Keywords: ultrafiltration, dye removal, complexation, polyoxometalates, permeate flux.

Abstract: To improve dye retention, there is a concurrent interest in the development and optimization of an alternative and promising method for the dye recovery in aqueous solutions. In this regard, considerable attention was paid to the polyoxometalates (POMs) assisted ultrafiltration (POMAUF). The aim of the present study is to eliminate toluidine blue (TB) dye by ultrafiltration membrane using keggin polyoxometalates (POMs) as complexing agents. In the first step, the keggin polyoxometalates $K_3[PW_{12}O_{40}]\cdot 6H_2O$ (PW_{12}) and $K_7[PW_{11}O_{39}]\cdot 14H_2O$ (PW_{11}) were prepared. Then, the obtained powders were characterized by X-ray diffraction and infrared spectroscopies. Afterwards, the removal of toluidine blue (TB) using polyoxometalates assisted ultrafiltration (POMAUF) was studied. Factors affecting the retention of dye and permeate flux such as transmembrane pressure, operating time, polyoxometalates concentration, ionic strength, surfactant and pH were investigated. All results of both compounds have been presented and discussed. The results reveal that the addition of POMs leads to an increase in dye retention from 11 to 95% for the PW_{12} and to 98% for the PW_{11}. The results of this work have thus suggested the promising enhancement of ultrafiltration membrane selectivity for the dye removal using new complexing agents such as POMs in place of polyelectrolytes and surfactants.

Introduction

Generally, the synthetic textile dyes depict a large family of organic compounds that could generate various and undesirable effects on the environment and this can be a serious risk to human health (Bazin et al. 2012). Indeed, it is known that synthetic dyes are used in many technological processes such as the textile industry, leather tanning, paper production, food technology, agriculture and hair coloring manufacture (Forgacs et al. 2004). The most frequently used industrial dyes are the azo, anthraquinone, indigoid, triphenylmethyl (trityl), and phthalocyanine derivatives, knowing that the azo dye is the most dominated classes (Forgacs et al. 2004). Thus, the increasing difficulty in treating textile dyes has led to a renewable research for new methods that are effectively and economically viable. Therefore, important treatment methods such as coagulation--flocculation, electrochemical oxidation, and adsorption and membrane filtration have been used to remove dye from wastewater. Indeed, the use of membrane to eliminate dye from aqueous solution is an advantage because no chemicals are added (Mukherjee et al. 2005, Van der Bruggen et al. 2001). The most known membrane filtration processes are the microfiltration (MF) (Van der Bruggen et al. 2001, Van der Bruggen et al. 2005), ultrafiltration (UF) (Buckley 1992, Porter 1998), nanofiltration (NF) and reverse osmosis (RO) (Akbari et al. 2002). Previously, the complexation-ultrafiltration method was considered as a promising technology for separation of micropollutants such as dye and heavy metals from effluents. Several experiments have been done using polyelectrolyte enhanced ultrafiltration (PEUF) for the removal of dyes (Dasgupta et al. 2015, Tan et al. 2006). In fact, the micellar enhanced ultrafiltration (MEUF) method was investigated by several authors. Purkait et al. (2004) have demonstrated that the retention of eosin increases substantially by adding the surfactant (CPC). In addition, Zaghbani et al. (2007) have found that the retention of MB reached 99% when SDS surfactant was added as complexing agent. Also, other studies used the MEUF process (Aroua and Zuki 2007, Baek et al. 2003, Juang et al. 2003).

On the other hand, polyoxometalates (POMs) are a large family of metal-oxide assemblies. They are constructed via the condensation of metal oxide polyhedral MO_x (M=W, Mo, V, etc. and x=4–7) with each other (Miras et al. 2012, Han et al. 2014). Indeed, what contributes to POMs' particularity is strong Brønsted acidity, strong oxidizing agents, a wide range of structures, combinations of metals and possible sizes, as well as a high solubility in water. Furthermore, they are negatively

charged and possess predominantly O^{2-} ligands. These properties have solved various environmental problems such as toxic gas sequestration, wastewater decontamination and dye removal (Errington et al. 2010, Hu et al. 2011, Niu et al. 2011).

In this context, several researches have been using the POMs in their studies. As an example, Omwoma et al. (2014) have been using POMs as photo catalysts for the removal of dyes and heavy metals from wastewater. Also, Bi et al. (2011) engineered the POM/LDH nanocomposite which was used to adsorb methylene blue dye from water. In addition, a new integrated approach for dye removal from wastewater by polyoxometalates functionalized membranes was done by Yao et al. (2016). They showed that the membrane integrating both the adsorptive and catalytic activities was developed by introducing polyoxometalates (POMs) as an ideal candidate for the membrane functionalization via a novel sol-gel method.

The purpose of this study is to apply the keggin polyoxometalates as complexing agents to remove TB dye from aqueous solution. To the best of our knowledge, it will be the first attempt of the application of POMs to enhance the ultrafiltration (UF) membrane selectivity for the treatment of dye wastewater. The retention rate and permeate flux were studied as a function of variable parameters such as time, pressure, POMs, salt and surfactant concentrations as well as pH value of the solution.

Experimentals

Chemicals

Toluidine Blue (TB) (molecular weight: 305.83 g·mol^{-1}, λ_{max}=623 nm, Fig. 1), cetyltrimethylammonium bromide (CTAB), sodium chloride, hydrochloric acid, sodium hydroxide, sodium tungestate, disodium hydrogen phosphate, acetic acid, potassium chloride were purchased from Fluka. All the chemicals were used without further treatment.

Synthesis of POMs

The anionic POMs type keggin of formula $K_3[PW_{12}O_{40}]\cdot 6H_2O$ (PW_{12}) with a molecular weight MW=3100 g·mol^{-1} and $K_7[PW_{11}O_{39}]\cdot 14H_2O$ (PW_{11}) (MW=3202.87 g·mol^{-1}) were used in the present work. The potassium salt of keggin type heteropolyanion was synthesized in the laboratory according to the modified methods described in the literature (Rocchiccioli--Deltcheff et al. 1983); $Na_2WO_4\cdot 2H_2O$ (100 mmol), Na_2HPO_4 (9.1 mmol), and acetic acid (60 mL) were mixed in 200 ml of deionized water. Then the mixture was stirred with a magnetic stirrer, while the temperature raised to 80–85ºC, potassium chloride KCl (45 mmol) was added dropwise to the solution. The white precipitate formed was filtered and then extracted with ether. The lacunary polyoxometallate PW_{11} salt was obtained by a direct method described by (Contant 1987); sodium tungstate dihydrate (181.5 g) was dissolved in 300 mL of distilled water. Phosphoric acid (50 ml) and acetic acid (88 ml) were successively added. The solution was refluxed for 60 min, and then 60 g of solid potassium chloride was added. A fine precipitate appeared which was filtered and dried in air. The successful formation of the anionic PW_{12} and $PW_{11}$was confirmed by FTIR and DRX analyses. The purity of the resulting powder was checked from the examination of its X-ray powder diagram collected on a PANalytical diffractometer using CuKα radiation (λ=1.5418 Å). The crystalline phase was determined by the comparison of the registered patterns with the International Center for Diffraction Data (ICDD)-Powder Diffraction Files (PDF). IR spectra were recorded by a Perkin Elmer (FTIR 2000) spectrometer in the range of 4000–400 cm^{-1} using KBr pellets. The UV-Vis spectra were carried out using Lambda-25 (Perkin Elmer) spectrophotometer in the wavelength range of 200–800 nm. All measurements were recorded at room temperature.

Ultrafiltration process

UF membrane

The ultrafiltration membrane used in this study was organic regenerated cellulose (RC) membrane with molecular weight cut-off (MWCO) 3 kDa and effective filtration area of 15.54 cm^2. The ultrafiltration membrane was provided by Millipore (Germany). Before use, the virgin membrane was soaked in deionized water for 24 hours. Then, the membrane was compacted for 3 hours under 3 bar pressure to eliminate preservative products.

The pure water membrane permeability was measured in order to ensure that the initial membrane Lp^o is restored. The pressure was ranging from 2 to 5 bar and the permeate flux was measured at each pressure value. Furthermore, the curve J=f(ΔP) was traced. The water permeability of the membrane was found to be Lp^o=10 L·h^{-1}·m^{-2} (Fig. 2). This Lp^o value is considered as a reference used to evaluate the cleaning procedure, concentration polarization and the fouling of the membrane.

Procedure

UF process was performed using an Amicon stirred batch cell (model 8050) (Millipore) connected to a nitrogen-pressurized solution reservoir. In each UF experiment, the concentration of TB was fixed at 0.1 mM, the feed solution was kept stirred

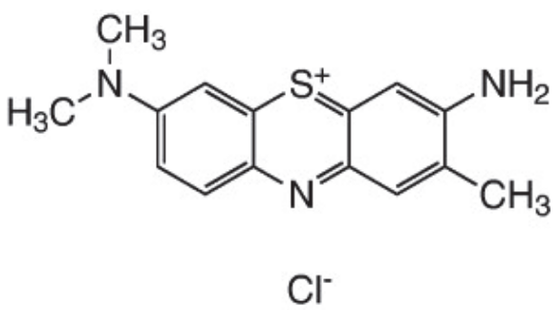

Fig. 1. Molecular structure of TB dye

at 300 rpm, the temperature was 25ºC and the pressure was maintained at 2.5 bars except for the pressure effect. The P/D molar ratio was fixed at 1 for the effect of time, pressure, salt, surfactant and pH.

For each UF manipulation, the permeate solution was collected after a flow time of 4 to 5 min to ensure an equilibrium state. Then, a permeate volume of 5 mL was collected and analyzed by UV-visible spectrophotometer. After each manipulation, the membrane was immediately washed with distilled water and the water flux was measured in order to assess the cleanness of the membrane. The pH solution was adjusted at the desired level by the addition of hydrochloric acid or sodium hydroxide solutions.

To evaluate the efficiency of the ultrafiltration process to remove the dye, two parameters, the permeate flux (J) and the retention rate (R%) are determined according to the Eqs. 1 and 2. The permeate flux was calculated as follows:

$$J = \frac{V}{\Delta t \cdot S} \quad (1)$$

Where J denotes the permeate flux ($L \cdot h^{-1} \cdot m^{-2}$), V is the volume of the permeate sample (L), Δt is the time difference (h), and S denotes the effective membrane surface area (m^2).

The filtration efficiency in removing dye from the feed solution was evaluated through the dye rejection which was calculated using the classical rejection coefficient:

$$R\% = \left(1 - \frac{C_p}{C_0}\right) \cdot 100 \quad (2)$$

Where C_0 is the initial concentration of the dye in the initial solution and C_p is the dye concentration in the permeate tank.

Results and discussion

X-ray-diffraction POMs

The registered X-ray-diffraction (XRD) pattern of PW_{12} and PW_{11} is shown in Figure 3. The parameters of the unit cell are determined by using the X'Pert High Score Plus program (JCPDS-file 00-034-0204). Figure 3a shows the pattern of PW_{12}, we found that all picks were indexed to a tetragonal phase with space group P4nc (n°104). The lattice parameters are: a=b=14,162 Å; c=12,533 Å; a=b=g=90° and Z=2. The registered XRD pattern of PW_{11} is shown in Figure 4b. All picks were indexed to a tetragonal phase with space group P4nc (n°104). The lattice parameters are: a=b=14,192 Å; c=12,528 Å; a=b=g=90° and Z=2.

Infrared spectroscopy

In order to get a better insight into the chemical bands in the inorganic compounds synthesized, FTIR measurement was used. Figure 4 shows the FTIR spectra of PW_{12} and PW_{11} anions. There can be observed the presence of bands at 715–741 cm^{-1}, 879–907 cm^{-1}, 861–966 cm^{-1} and 1061–1075 cm^{-1} (Tab. 1). These bands are attributed to the ν_{as}(W-O_c-W), ν_{as}(W-O_b-W), ν_{as}(W-O_t) (terminal oxygen linked to alone tungsten atom) and ν_{as}(P-O_a) (the central tetrahedral PO_4 bonds in the ions) links, respectively. The O_b and O_c are the corner shared oxygen atoms and the edge shared oxygen atoms of WO_6 octahedra, respectively (You et al. 2010). All the absorption band frequencies of this compound were typical keggin anion skeletal vibrational bands. The broad absorption band around 3440 cm^{-1} is attributed to the n(OH) vibration and the band located at 1616 cm^{-1} is relative to the deformation of water molecule δ(H_2O). They indicate that the POMs accommodate a large amount of water of crystallization as well as the H^+ (Chen et al. 2008). In the IR spectrum of the PW_{11} the absorption bands are very similar to those of the PW_{12} and the decrease in the intensity of the ν_{as}(W-O_t) vibration indicates a loss of the W=O_t. Thus, the observed XRD patterns and the vibrational spectra are in good agreement.

Absorption spectra

The absorption spectra of both POMs are recorded in the UV region from 200 to 400 nm and presented in Figure 5. The spectra present the characteristic of the maximum absorption band around 250 nm for PW_{12} and PW_{11}. They are attributed to the O→W charge transfer transition of the keggin unit at the W=O bond and W–O–W bond (Santos et al. 2015).

Ultrafiltration study

TB retention as function of time

Figure 6a presents the retention of dye versus the time in the absence and in the presence of POMs. It can be seen from

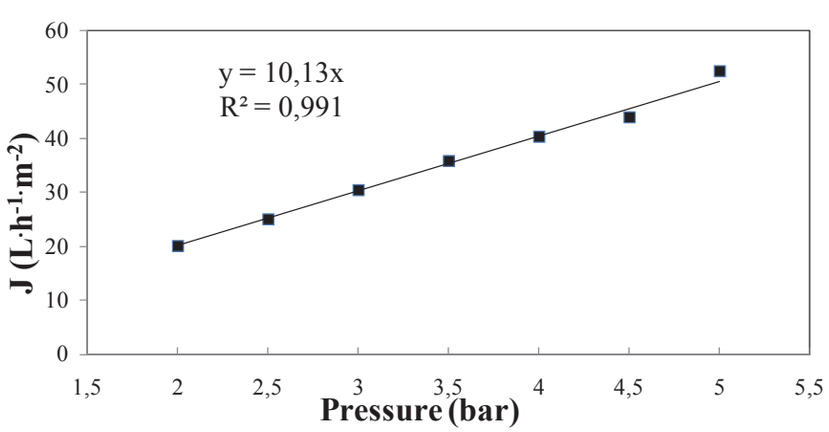

Fig. 2. Permeate flux of water as a function of pressure

this Figure that the UF membrane is unable to retain the TB molecules. Thus the retention remained almost constant at the value of 11%. This modest retention may be attributed to the adsorption of dye at the surface or in the pores of the membrane (Fradj et al. 2014).

On the other hand, the addition of POMs improves significantly the dye retention, which increases to 98% in the case of PW_{11} and to 95% in the case of PW_{12} (blue curve). So it is clear that the retention of dye was independent of the time period examined in both cases (absence and presence of POMs).

Figure 6b presents the variation of permeate flux as a function of time. It can be shown from the spectra that the permeate flux declined over time. It is also evident to remark that the permeate flux was higher for the dye solution as compared to the POMs/TB complex. In fact, in the absence of POMs, the aggregate formation of dye onto the membrane surface was less noticeable, since the dye particle could easily pass through the membrane. Thus, this reduced the resistance against the solvent flux through the membrane. However, after the addition of POMs, most of the complexes formed were retained over the membrane surface. Such behavior can be explained in the following way: the (POMs/dye) complexes generate deposited layer over the membrane surface and consequently decrease the permeate flux compared to that of the dye solution. The same trends have been reported by Fradj et al. (2014) and Zaghbani et al. (2007).

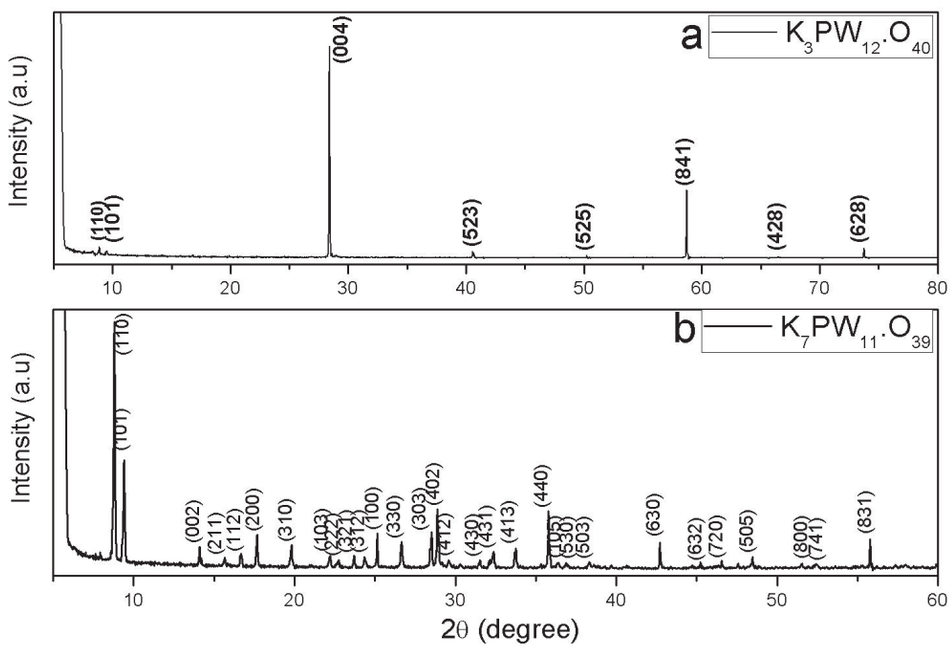

Fig. 3. XRD patterns of PW_{12} (a) and PW_{11} (b)

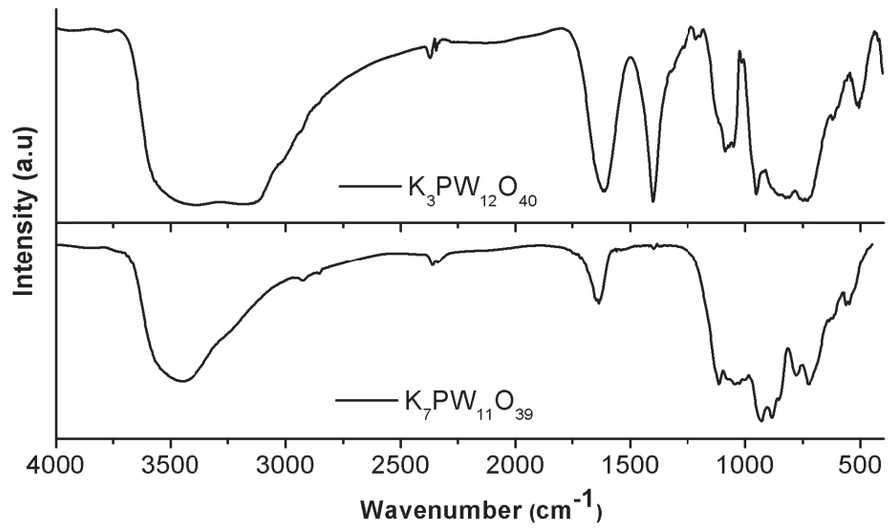

Fig. 4. IR spectra of PW_{12} and PW_{11} recorded at room temperature in the range of 4000–400 cm^{-1}

Pressure effect

The variation of the dye rejection against pressure is presented in Figure 7. The pressure ΔP was ranging from 1 to 4 bars. As shown from Figure 7a, the dye rejection has a slight variation as a function of the pressure increases (black curve). However, in the case of POMs/TB complexes, the retention of dye is improved and made stable in all the range of pressure. Such behavior was found by Huang et al. (2010) and Zaghbani et al. (2007). However, it can be seen from Figure 8a that the dye retention reached 98% (PW_{11}) and 95% (PW_{12}). This behavior may indicate that the retention of dye by POMs is mainly induced by the electrostatic interaction between the POMs and the dye.

The permeate flux versus operating pressure was plotted in Figure 7b. As shown from this Figure the flux increases with increasing pressure value (all curves). Indeed, an advanced explanation described by Ahmad and Puasa (2007) reveals that the effective driving force for the solvent

Table 1. IR frequencies (cm^{-1}) and their assignments

IR (cm^{-1})				Attributions
$K_7PW_{11}O_{39}$	Intensity	$K_3PW_{12}O_{40}$	Intensity	
3450	vs	3407	vs	v (O-H)
		3161	vs	
1114	vs	1082	vs	$v_{as}(P\text{-}O_a)$
1043				
935	m	940	m	$v_{as}(W\text{-}O_t)$
877				
783	m	818	m	$v_{as}(W\text{-}O_b\text{-}W)$
720	m	741	m	$v_{as}(W\text{-}O_c\text{-}W)$
631	sh	621	vw	
555	vw			

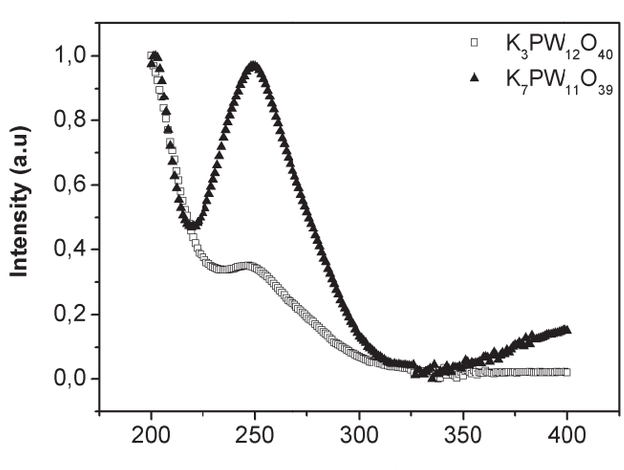

Fig. 5. Absorption spectra of PW_{12} and PW_{11} recorded at room temperature in the range of 200–400 nm

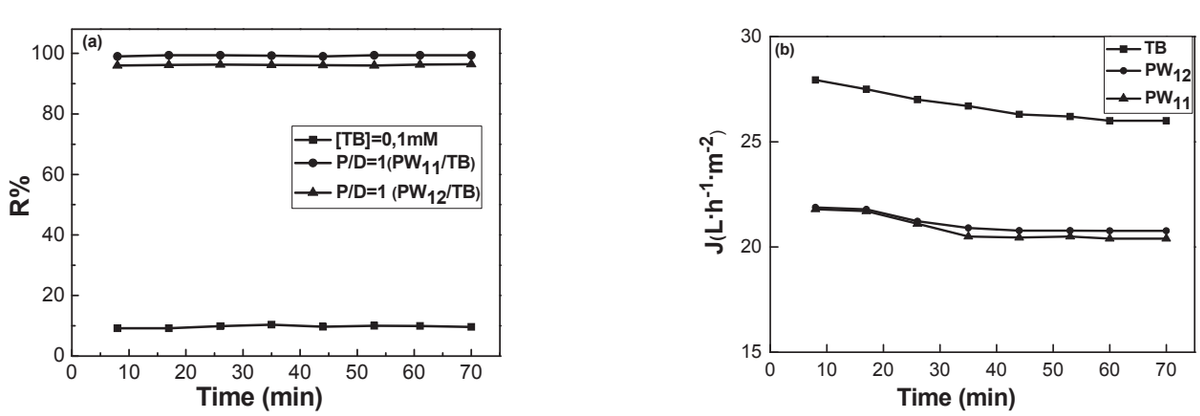

Fig. 6. Time effect of (a) retention of TB and (b) permeate flux

transport is becoming higher as a function as pressure increases. Furthermore, the increase in the driving force will overcome the membrane resistance and more water passes through the membrane leading to higher permeate flux. Our results are in concordance with literature (Ouniand Dhahbi 2010a, Hammami et al. 2016).

POMs concentration effect

The effect of POMs on the TB retention and permeate flux was investigated for POMs concentration ranging from 0 to 1 mM.

As can be seen from Figure 8a, at low PW_{12} concentrations equal to 0.01, 0.02 and 0.05 mM the obtained dye retention is 20%, 26%, 74%, respectively. In the case of PW_{11}, the concentration of 0.01, 0.02 and 0.05 mM leads to 16%, 27% and 95% dye retention, respectively. However, when the concentration reaches 0.1 mM, the dye retention reaches 95% for PW_{12} and 98% for PW_{11}. Meanwhile, the color of the solution in the permeate tank underwent an obvious variation, from blue to transparent. This behavior may be explained as a maximum retention obtained when there are a sufficient number of polyoxometalates sites available to bind almost all of the dye molecules. The maximum dye rejection was achieved from POM/dye ratio of 1:1 for both polyanions. These results are in good agreement with other studies which have shown that the addition of polyelectrolyte and surfactant improved significantly the retention of dyes (Ouni and Dhahbi 2010b, Purkait et al. 2004) as well as heavy metals (Haktanır et al. 2017, Huang et al. 2010). In addition, it is worth to point out that the retention of TB dye is greater in the case of PW_{11}. This result can be explained by the fact that the lacunary PW_{11} has higher charges and therefore a higher nucleophilicity compared to the PW_{12}. Thus, they react quite easily with the dye molecules in water solution. Furthermore, Yin et al. (2012) pointed out that at dissolving POMs, the clusters interact electrostatically with other species, thus leading to chemical associations between POMs and cationic ions, molecules, complexes and polymers. In addition, several researchers have indicated in their studies that POMs can interact with proton donors trough hydrogen bonds, in ammonium analogues (Akutagawa et al. 2011) and proteins (Zhang et al. 2007, Zhou et al. 2011).

Figure 8b presents the variation of the permeate flux as a function of the POM concentration. From this Figure, it is clearly seen that for both POMs the permeate flux has slightly declined over. The resulting complex forming a gel--layer covering the surfaces of the membrane will affect the permeation flux. The same trend has been reported by (Baek et al. 2003, Haktanır et al. 2017).

Ionic strength effect

The effects of ionic strength on the TB removal and permeate flux were studied at different NaCl concentrations ranging from 0.01 to 1500 mM as illustrated in Figure 9.

Indeed, from Figure 9a, it can be deduced that at low salt concentration ranging from 0.01 mM to 10 mM, the bond which forms between the POMs and the dyes remains stable, thus we have a significant retention of dye.

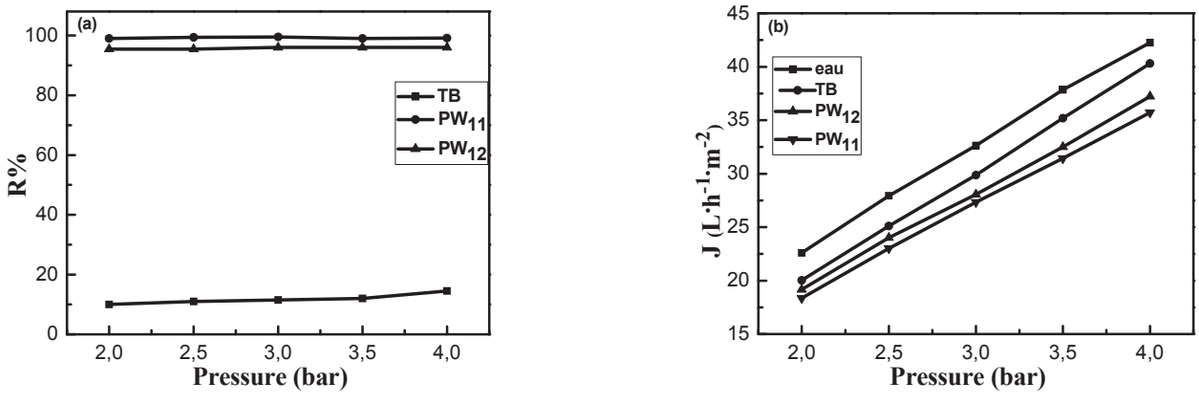

Fig. 7. Effect of transmembrane pressure on (a) TB retention and (b) permeate flux

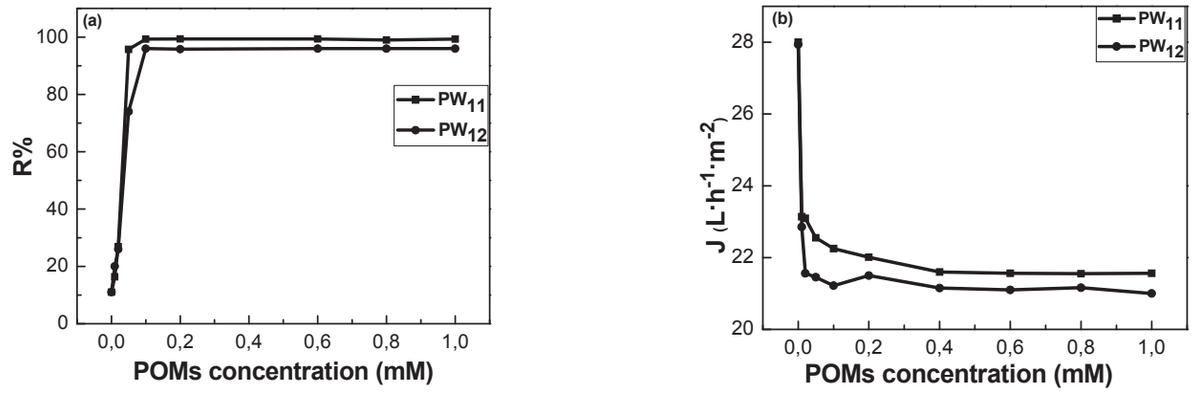

Fig. 8. Variation of (a) TB retention and (b) permeate flux as a function of feed POMs concentration

However, the increase of salt concentration from 100 to 1500 mM leads to the decrease of dye elimination from 98 to 93% in the case of PW_{11} and from 95 to 92% in presence of PW_{12}.

Such behaviors can be explained accordingly:

- It seems that a competition between Na^+ and TB^+ occurs at the same binding sites on the POMs surface.
- The release of the dye molecules in solution leads to its passage through the UF membrane (Hammami et al. 2016).

By comparison with the literature, our results are similar to those obtained by (Hammami et al. 2016, Verbych et al. 2006).

On the other hand, the variation of permeate flux as a function of the feed concentration of sodium chloride is shown in Figure 9b. It is clearly observed that the permeate flux decreased slightly when the concentration of NaCl increased. An advanced explanation made by (Huang et al. 2010) shows that the complex aggregations are formed at the membrane surface which enhance the effect of polarization concentration.

Surfactant effect

Given that industrial effluents contain a surfactant mixture that is not readily biodegradable and may complicate the dye retention, several studies have been done to improve the dye retention. So, in this case the effect of CTAB surfactant on the dye removal and on the permeate flux was investigated (Fig. 10). In fact, it is worth noting that the CTAB concentration ranged from 0.001 to 10 mM.

Generally, the addition of surfactant to an aqueous solution with concentration more than the critical micelle concentration (CMC) leads to the formation of large amphiphilic aggregate micelles. Thus, the dissolved entities can be mostly trapped by the micelles surface and will be solubilized (Zhang et al. 2009).

It can be observed from Figure 10a that for low CTAB concentration of 0.001 and 0.01 mM, the retention rate slightly decreases, but remains important in order to 96 and 97% for PW_{12} (red curve) and PW_{11} (black curve), respectively. Whereas for a CTAB concentration of 1 mM and 10 mM, the dye retention decreases sharply to 12% and 11% for both POMs. This behavior may be explained thus:

At lower CTAB concentrations, CTA^+ interact partially with POMs negative site, but there are enough sites for binding TB^+.

- However, when CTAB increases, the negative site on the POM surface is progressively saturated, the counter--ions at the surface of POM anions are replaced by the cationic amphiphiles CTA^+. This results in the formation of hydrophilic POMs core that is surrounded by the hydrophobic shell with alkyl chains outside the surface (Verbych et al. 2006, Zhang et al. 2009).
- Consequently, the dye molecules become free in solution and easily pass through the pores of the membrane which explains the retention drop.

The variation of permeate flux as a function of feed concentration of surfactant is presented in Figure 10b. As shown, the permeate flux slightly decreases when the concentration of CTAB increases. It is worth pointing out that the flux decline is most probably caused by the gel layer formation and an increase in solvent viscosity.

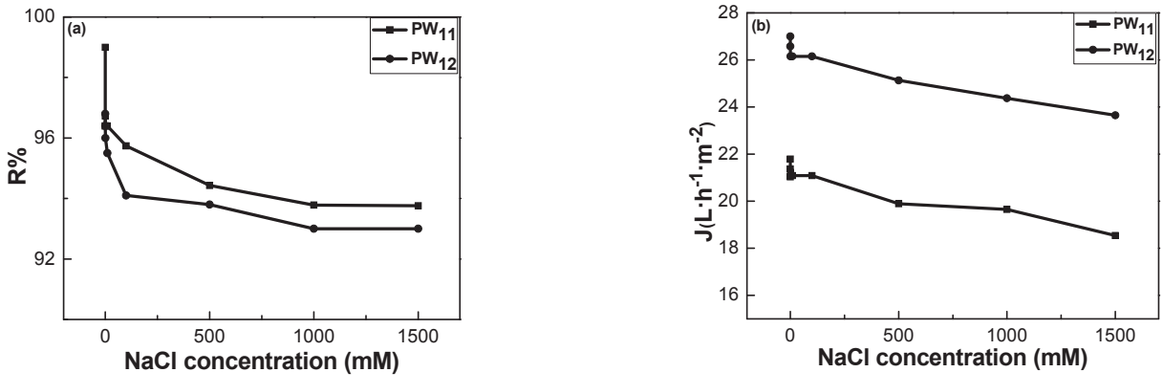

Fig. 9. Variation of (a) TB retention and (b) permeate flux as a function of feed NaCl concentration

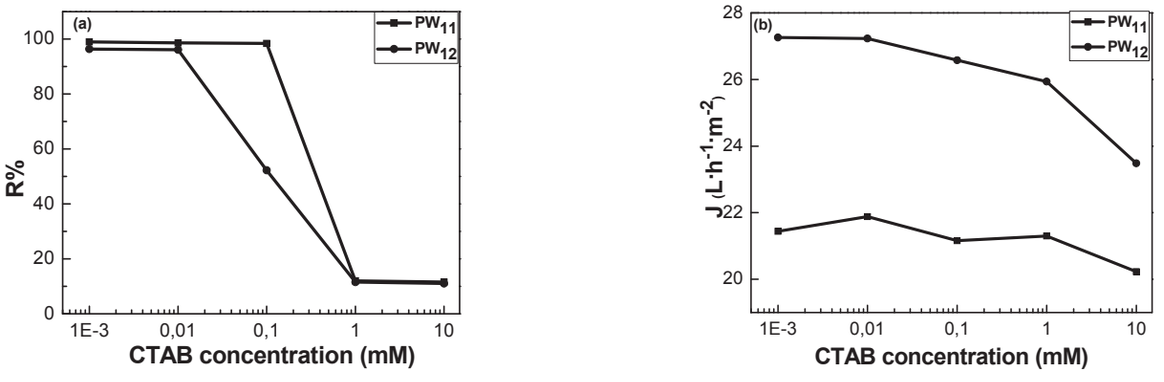

Fig. 10. Variation of (a) TB retention and (b) permeate flux as a function of feed surfactant concentration

pH effect

The effect of pH on the TB retention and on the permeate flux is depicted in Figure 11. The pH value is ranging from 2 to 12 by adding appropriate amounts of hydrochloric acid or sodium hydroxide (0.1 M).

It can be seen from Figure 11a that the high retention of TB molecules was persisted at wide pH range of 2–12. In fact, previous research has found that POMs in aqueous solution decomposes in a stepwise fashion with increasing pH. In the first step at pH<8, PW_{12} decomposes partially with the removal of W=O units to give the following species $[P_2W_{21}O_{71}]^{6-}$ + $[PW_{11}O_{39}]^{7-}$ (at pH=2.2), $[PW_{12}O_{40}]^{3-}$ + $[P_2W_{21}O_{71}]^{6-}$ + $[PW_{11}O_{39}]^{7-}$ + $[P_2W_{18}O_{62}]^{6-}$ + $[P_2W_{19}O_{67}]^{10-}$ (at pH=3.5), $[P_2W_{21}O_{71}]^{6-}$ + $[PW_{11}O_{39}]^{7-}$ + $[P_2W_{18}O_{62}]^{6-}$ (at pH=5.4) and $[PW_9O_{34}]^{9-}$ (at pH=7.3). In the second step at pH>8, tungstophosphoric completely decomposes to PO_4^{3-} and WO_4^{2-} (Zhu et al. 2003). Above pH=8, there may be formation of tungsten hydroxide $[WO_4(OH)_n]^{(n+2)-}$ (Mahadevaiah et al. 2007). This colloidal precipitate blocks the pores of the membrane and prevents the passage of the dye. As a consequence the dye retention remains high.

Compared with previously published results (Ouni and Dhahbi 2010a, b), the present study presents a significant dye removal in both acidic as well as alkaline pH values.

On the other hand, the variation of permeate flux as a function of pH values is presented in Figure 11b. From this figure, it can be seen that the flux maintained stable throughout the range of pH value.

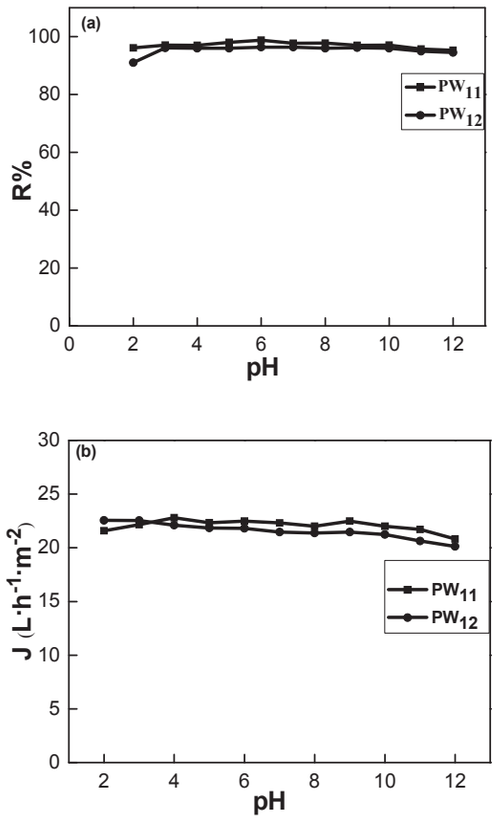

Fig. 11. Variation of (a) TB retention and (b) permeate flux as a function of pH

Conclusion

The results of this study have distinctly evinced that the polyoxometalates assisted ultrafiltration (POMAUF) process is a promising method for the TB removal.

The obtained results clearly suggest that:

- The retention of TB increases progressively with the increase of POMs concentration and reaches the maximum value of 95% and 98% for PW_{12} and PW_{11}, respectively.
- The applied transmembrane pressure and the operating time have no influence on the dye retention. This means that the interaction between the POMs and the dye molecules was only responsible for the removal of dye.
- The retention of the dye decreases by the addition of high concentration of NaCl and CTAB. This is due to a competition between the molecules of TB^+ and the ions Na^+ or CTA^+ on the same negative sites on the POMs surface.
- The retention of dye remains high in a broad range of pH values ranging from 2 to 12.

In light of the results obtained, it can be argued that polyoxometalates-assisted ultrafiltration may be a promising new method for removing various pollutants from effluents.

Acknowledgements

The authors wish to acknowledge the Head of the Department of Chemistry and Laboratory of Water, Membrane and Environmental Biotechnology (LEMBE) CERTE of Tunisia and all who supported and assisted in conducting this study.

References

Ahmad, A.L. & Puasa, S.W. (2007). Reactive dyes decolourization from an aqueous solution by combined coagulation/micellar-enhanced ultrafiltration process, *Chemical Engineering Journal*, 132, pp. 257–265, DOI: 10.1016/j.cej.2007.01.005.

Akbari, A., Desclaux, S., Remigy, J.C. & Aptel, P. (2002). Treatment of textile dye effluents using a new photografted nanofiltration membrane, *Desalination*, 149, pp. 101–107, DOI: 10.1016/S0011-9164(02)00739-7.

Akutagawa, T., Kudo, F. & Tsunashima, R. (2011). Hydrogen-bonded assemblies of two-electron reduced mixed-valence $[XMo_{12}O_{40}]$ (X=P and Si) with p-phenylenediamines, *Inorganic Chemistry*, 50, pp. 6711–6718, DOI: 10.1021/ic200683e.

Aroua, M.K. & Zuki, F.M. (2007). Removal of chromium ions from aqueous solutions by polymer-enhanced ultrafiltration, *Journal of Hazardous Materials*, 147, pp. 752–758, DOI: 10.1016/j.jhazmat.2007.01.120.

Baek, K., Kim, B.K., Cho, H.J. & Yang, J.W. (2003). Removal characteristics of anionic metals by micellar-enhanced ultrafiltration, *Journal of Hazardous Materials*, 99, pp. 303–311, DOI: 10.1016/S0304-3894(03)00063-3.

Bazin, I., Ibn Hadj Hassine, A., Haj Hamouda, Y., Mnif, W., Bartegi, A., Ferber, M.L., De Waard, M. & Gonzalez, C. (2012). Estrogenic and anti-estrogenic activity of 23 commercial textile dyes, *Ecotoxicology and Environmental Safety*, 85, pp. 131–136, DOI: 10.1016/j.ecoenv.2012.08.003.

Bi, B., Xu, L., Xu, B. & Liu, X. (2011). Heteropoly blue-intercalated layered double hydroxides for cationic dye removal from aqueous media, *Applied Clay Science*, 54, pp. 242–247, DOI: 10.1016/j.clay.2011.09.003.

Buckley, C.A. (1992). Membrane technology for the treatment of dye house effluents, *Water Science Technology*, 25, 10, pp. 203–209.

Chen, J., Dong, W., Möhwald, H. & Krastev, R. (2008). Amplified fluorescence quenching of self-assembled polyelectrolyte-dye nanoparticles in aqueous solution, *Chemistry of Materials*, 20, pp. 1664–1666, DOI: 10.1021/cm071678h.

Contant, R. (1987). Relationships between apparent tungsto phosphates with the anion $PW_{12}O_{40}^{3-}$. Synthesis and proprieties of a new lacunary polyoxotungstophosphate $K_{10}P_2W_{20}O_{70}{\cdot}24H_2O$, *Canadian Journal of Chemistry*, 65, pp. 568–573. (in French)

Dasgupta, J., Singh, M., Skider, J., Padarthi, V., Chakraborty, S. & Curcio, S. (2015). Ecotoxicology and environmental safety response surface-optimized removal of Reactive Red 120 dye from its aqueous solutions using polyethyleneimine enhanced ultrafiltration, *Ecotoxicology and Environmental Safety*, pp. 1–8, DOI: 10.1016/j.ecoenv.2014.12.041.

Errington, R.J., Coyle, L., Middleton, P.S., Murphy, C.J., Clegg, W. & Harrington, R.W. (2010). Synthesis and structure of the alkoxido--titanium pentamolybdate $({}^{n}Bu_4N)_3[({}^{i}PrO)TiMo_5O_{18}]$: An entry into systematic $TiMo_5$ reactivity, *Journal of Cluster Science*, 21, pp. 503–514, DOI: 10.1007/s10876-010-0329-3.

Forgacs, E., Cserháti, T. & Oros, G. (2004). Removal of synthetic dyes from wastewaters: A review, *Environment International*, 30, pp. 953–971, DOI: 10.1016/j.envint.2004.02.001.

Fradj, A.B., Hamouda, S.B., Ouni, H., Lafi, R., Gzara, L. & Hafiane, A. (2014). Removal of methylene blue from aqueous solutions by poly(acrylic acid) and poly(ammonium acrylate) assisted ultrafiltration, *Separation and Purification Technology*, 133, pp. 76–81, DOI: 10.1016/j.seppur.2014.06.038.

Haktanır, C., Özbelge, H.Ö., Bıçak, N. & Yılmaz, L. (2017). Removal of hexavalent chromium anions via polymer enhanced ultrafiltration using a fully ionized polyelectrolyte, *Separation Science and Technology (Philadelphia)*, 52, pp. 2487–2497, DOI: 10.1080/01496395.2017.1343351.

Hammami, M., Ennigrou, D.J., Naifer, K.H. & Ferid, M. (2016). Recovery of samarium (III) from aqueous solutions by poly(sodium 4-styrenesulfonate) assisted-ultrafiltration, *Environmental Progress & Sustainable Energy*, 35, 4, pp. 1–7, DOI: 10.1002/ep12335.

Han, X., Zhang, Z., Zhang, T., Li, Y.G., Lin, W., You, W., Su, Z.M. & Wang, E.B. (2014). Polyoxometalate-based cobalt-phosphate molecular catalysts for visible light-driven water oxidation, *Journal of the American Chemical Society*, 136, 14, pp. 5359–5366, DOI: 10.1021/ja412886e.

Hu, Y., Luo, F. & Dong, F. (2011). Design synthesis and photocatalytic activity of a novel lilac-like silver-vanadate hybrid solid based on dicyclic rings of $[V_4O_{12}]^{4-}$ with $\{Ag_7\}^{7+}$ cluster, *Chemical Communications*, 47, pp. 761–763, DOI: 10.1039/C0CC02965C.

Huang, J.H., Zhou, C.F., Zeng, G.M., Li, X., Niu, J., Huang, H.J., Shi, L.J. & He, S.B. (2010). Micellar-enhanced ultrafiltration of methylene blue from dye wastewater via a polysulfone hollow fiber membrane, *Journal of Membrane Science*, 365, pp. 138–144, DOI: 10.1016/j.memsci.2010.08.052.

Juang, R.S., Xu, Y.Y. & Chen, C.L. (2003). Separation and removal of metal ions from dilute solutions using micellar-enhanced ultrafiltration, *Journal of Membrane Science*, 218, pp. 257–267, DOI: 10.1016/S0376-7388(03)00183-2.

Mahadevaiah, N., Venkataramani, B. & Prakash, B.S.J. (2007). Restrictive entry of aqueous molybdate species into surfactant modified montmorillonite – a breakthrough curve study, *Chemistry of Materials*, 19, pp. 4606–4612, DOI: 10.1021/cm071028d.

Miras, H.N., Yan, J., Long, D.L. & Cronin, L. (2012). Engineering polyoxometalates with emergent properties, *Chemical Society Reviews*, 41, p. 7403, DOI: 10.1039/c2cs35190k.

Mukherjee, P., Jones, K.L. & Abitoye, J.O. (2005). Surface modification of nanofiltration membranes by ion implantation, *Journal of Membrane Science*, 254, pp. 303–310, DOI: 10.1016/j.memsci.2005.01.004.

Niu, J., Zhang, S., Chen, H., Zhao, J., Ma, P. & Wang, J. (2011). 1-D, 2-D, and 3-D organic-inorganic hybrids assembled from keggin--type polyoxometalates and 3d-4f heterometals, *Crystal Growth & Design*, 11, pp. 3769–3777, DOI: 10.1021/cg2001249.

Omwoma, S., Gore, C.T., Ji, Y., Hu, C. & Song, Y.F. (2014). Environmentally benign polyoxometalate materials, *Coordination Chemistry Reviews*, 286, pp. 17–29, DOI: 10.1016/j.ccr.2014.11.013.

Ouni, H. & Dhahbi, M. (2010a). Spectrometric study of crystal violet in presence of polyacrylic acid and polyethylenimine and its removal by polyelectrolyte enhanced ultrafiltration, *Separation and Purification Technology*, 72, pp. 340–346, DOI: 10.1016/j.seppur.2010.03.003.

Ouni, H. & Dhahbi, M. (2010b). Removal of dyes from wastewater using polyelectrolyte enhanced ultrafiltration (PEUF), *Desalination and Water Treatment*, 22, pp. 355–362, DOI: 10.5004/dwt.2010.1234.

Porter, J.J. (1998). Recovery of polyvinyl alcohol and hot water from the textile wastewater using thermally stable membranes, *Journal of Membrane Science*, 151, pp. 45–53, DOI: 10.1016/S0376-7388(98)00236-1.

Purkait, M.K., DasGupta, S. & De, S. (2004). Removal of dye from wastewater using micellar-enhanced ultrafiltration and recovery of surfactant, *Separation and Purification Technology*, 37, pp. 81–92, DOI: 10.1016/j.seppur.2003.08.005.

Rocchiccioli-Deltcheff, C., Fournier, M., Franck, R. & Thouvenot, R. (1983). Vibrational investigations of polyoxometalates. 2. Evidence for anion-anion interactions in molybdenum(VI) and tungsten(VI) compounds related to the keggin structure, *Inorganic Chemistry*, 22, pp. 207–216, DOI: 10.1021/ic00144a006.

Santos, F.M., Brandão, P., Félix, V., Nogueira, H.I.S. & Cavaleiro, A.M.V. (2015). Synthesis and properties of new materials with cobalt(II), iron(III) and manganese(III)-substituted keggin polyoxotungstates and 1-alkyl-3-methylimidazolium cations, *Polyhedron*, 101, pp. 109–117, DOI: 10.1016/j.poly.2015.07.032.

Tan, X., Kyaw, N.N., Teo, W.K. & Li, K. (2006). Decolorization of dye-containing aqueous solutions by the polyelectrolyte--enhanced ultrafiltration (PEUF) process using a hollow fiber membrane module, *Separation and Purification Technology*, 52, pp. 110–116, DOI: 10.1016/j.seppur.2006.03.028.

Van der Bruggen, B., Cornelis, G., Vandecasteele, C. & Devreese, I. (2005). Fouling of nanofiltration and ultrafiltration membranes applied for wastewater regeneration in the textile industry, *Desalination*, 175, pp. 111–119, DOI: 10.1016/j.desal.2004.09.025.

Van der Bruggen, B., Daems, B., Wilms, D. & Vandecasteele, C. (2001). Mechanisms of retention and flux decline for the nanofiltration of dye baths from the textile industry, *Separation and Purification Technology*, 22, pp. 519–528, DOI: 10.1016/S1383-5866(00)00134-9.

Verbych, S., Bryk, M. & Zaichenko, M. (2006). Water treatment by enhanced ultrafiltration, *Desalination*, 198, pp. 295–302, DOI: 10.1016/j.desal.2005.12.029.

Yao, L., Zhang, L., Wang, R., Chou, S. & Dong, Z. (2016). A new integrated approach for dye removal from wastewater by polyoxometalates functionalized membranes, *Journal of Hazardous Materials*, 301, pp. 462–470, DOI: 10.1016/j.jhazmat.2015.09.027.

Yin, P., Li, D. & Liu, T. (2012). Solution behaviors and self-assembly of polyoxometalates as models of macroions and amphiphilic polyoxometalate-organic hybrids as novel surfactants, *Chemical Society Reviews*, 41, p. 7368, DOI: 10.1039/c2cs35176e.

You, Y., Gao, S., Xu, B., Li, G. & Cao, R. (2010). Self-assembly of polyoxometalate-azure a multilayer films and their photocatalytic

properties for degradation of methyl orange under visible light irradiation, *Journal of Colloid and Interface Science*, 350, pp. 562–567, DOI: 10.1016/j.jcis.2010.07.001.

Zaghbani, N., Hafiane, A. & Dhahbi, M. (2007). Separation of methylene blue from aqueous solution by micellar enhanced ultrafiltration, *Separation and Purification Technology*, 55, pp. 117–124, DOI: 10.1016/j.seppur.2006.11.008.

Zhang, G., Keita, B., Craescu, C.T., Miron, S., Oliveira, P.D. & Nadjo, L. (2007). Polyoxometalate binding to human serum albumin: a thermodynamic and spectroscopic approach, *Journal of Physical Chemistry B*, 111, pp. 11253–11259, DOI: 10.1021/JP072947U.

Zhang, T., Brown, J., Oakley, R.J. & Faul, C.F.J. (2009). Towards functional nanostructures: ionic self-assembly of polyoxometalates and surfactants, *Current Opinion in Colloid and Interface Science*, 14, pp. 62–70, DOI: 10.1016/j.cocis.2007.10.003.

Zhou, Y., Zheng, L., Han, F., Zhang, G., Ma, Y., Yao, J., Keita, B., Oliveira, P.D. & Nadjo, L. (2011). Inhibition of amyloid-β protein fibrillization upon interaction with polyoxometalates nanoclusters, *Colloids and Surfaces A: Physicochemical and Engineering Aspects*, 375, pp. 97–101, DOI: 10.1016/j.colsurfa.2010.11.068.